Chapter 20
Electrospun Mixed Oxide-Based Composites as Cathodes for Lithium-Ion Batteries

Satishkumar R. Naik, Anand I. Torvi, and Mahadevappa Y. Kariduraganavar

20.1 Electrospinning Technique for Lithium-Ion Batteries—An Overview

Energy conversion and storage devices have drawn significant attention owing to depletion of fossil fuels, climate change and environmental deterioration. The commercialization of lithium-ion batteries (LIBs) was achieved in the early 1990s by employing an intercalated lithium metal oxide compound as a cathode and graphite as an anode material. However, the rapidly growing market for electric vehicles has created a demand for high energy storage capacity and fast charge/discharge capability with high energy density and durability. To meet these requirements, much research has been focused on improving the performance of pre-existing electrodes and/or developing new electrode materials. Novel nanofiber technologies particularly created the opportunity to design new materials for advanced rechargeable lithium-ion batteries. Currently, much effort has been devoted in developing nanostructure materials by employing various techniques, such as sol-gel method [1], wet chemical synthesis [2], chemical vapor deposition [3], the molten salt method [4–9], polymer precursor method [10–15] and electrospinning. Among these methods, electrospinning is a versatile, efficient and low-cost method, and has been used widely to synthesize nanofibers (NFs) with different morphologies. The electrospun NFs play a crucial role in various energy storage devices because of high surface area, controllable porosity and ease of accessibility.

S. R. Naik · A. I. Torvi · M. Y. Kariduraganavar (✉)
Department of Chemistry, Karnatak University, Dharwad 580003, India
e-mail: mahadevappayk@gmail.com

N. T. M. Balakrishnan and P. Raghavan (eds.), *Electrospinning for Advanced Energy Storage Applications*, Materials Horizons: From Nature to Nanomaterials,
https://doi.org/10.1007/978-981-15-8844-0_20

483331_1_En_20_Chapter ☑ TYPESET ☐ DISK ☐ LE ☑ CP Disp.:28/12/2020 Pages: 581 Layout: T1-Standard

20.2 Electrospinning

Electrospinning is a widely used fabrication technique for developing continuous electro-active nanofibers from a wide range of materials with diameters in the range of several nanometers to the micrometer regime. Among the different materials, nanofibers can be successfully obtained by electrospinning from polymers, semiconductors, ceramics, and their composites. Because of the decrease in the fiber diameter to nanoscale, these materials show enhanced properties of high surface area to volume ratio, porosity, flexibility, electrochemical and mechanical properties, which make them excellent candidates for a wide range of applications, such as energy conversion and storage devices, electronic devices and tissue engineering, etc.

20.2.1 Principle of Electrospinning

The basic principle behind the processing of nanofibers by electrospinning is based on the unidirectional elongation of a spinnable visco-elastic solution by considering various parameters involved in the process of electrospinning. Continuous nanofibers are formed due to the electrostatic Coulombic repulsive forces applied during elongation of the visco-elastic solution. The schematic representation of the electrospinning set-up is shown in Fig. 20.1. During the process of electrospinning, a visco-elastic solution is first loaded into a syringe and fed through a flow meter pump. When a high electric potential is applied to the spinnable solution at a threshold voltage of ~ 6 kV, the repulsive force developed in the electro-active solution is greater than its surface tension and a droplet, namely a Taylor cone, is formed at the tip of the syringe [16, 17]. This droplet is further elongated owing to electrostatic forces, which results in evaporation of the solvent and formation of solidified nanofibers, which are usually collected randomly on the grounded static/rotating mandrel collector substrate.

20.2.2 Parameters of Electrospinning

Electrospinning of fibers is influenced by various parameters. Some of the important parameters are briefly discussed below:

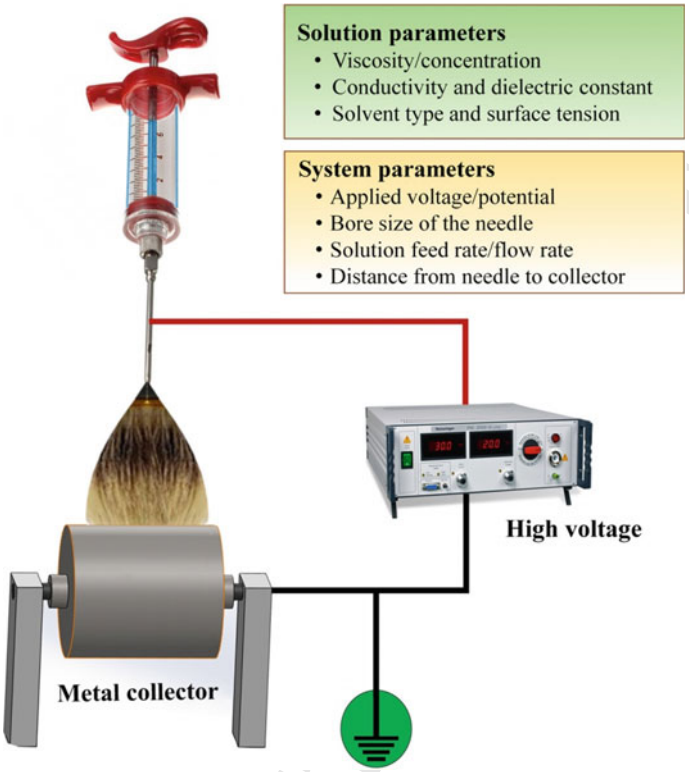

Fig. 20.1 Schematic representation of the electrospinning process

20.2.2.1 Process Parameters

Collector

The physical properties of electrospun fibers such as crystal morphology and molecular orientation are affected by the nature of collectors. Generally, a rotating drum collector is used as a collector. The diameter of the fibers can be controlled by monitoring the drum rotating speed. In some cases, the rotating disk is also used to develop uniaxially aligned fibers. The speed of collector could improve the crystal orientation of fibers due to polymer molecular chains' alignment in the direction of the fiber axis.

Applied Voltage

The applied voltage plays an important role in fiber development. An increase or a decrease in applied voltage can cause a change of morphology and structure of fibers. Increasing the voltage can cause an increase in the spinning current [18]. Increasing

spinning current can lead to an incidence of beaded morphology, and this structure can reduce the surface area. The studies have shown that the increase in voltage leads to an increase in fiber length and decrease in fiber size [19–21].

Distance Between Nozzle to Collector

The distance between nozzle and collector has a direct influence on morphology, structure, physical and chemical properties of the electrospun fibers. The studies show that by decreasing the distance between the nozzle and the collector, results in electrospun fiber with beaded structure and some cases, the shape of the fibers changed from circular to flat shape [19, 21].

Dispersion Flow Rate

The change in the rate of polymer flow from the syringe of electrospinning unit causes change in morphology, physical and chemical properties of the fibers. With increasing the flow rate, the diameter of the fiber could be increased and leads to beaded morphology [22–24].

20.2.2.2 *Solution Parameters*

Solution Concentration

The variation in the viscosity and surface tension of the polymer solution influences the spinning of fibers and controls the fiber structure and morphology. Low concentration solution generally forms droplets due to the influence of surface tension, while higher concentration prohibits fiber formation due to higher viscosity.

Volatility of Solvent

Electrospinning technique involves phase separation and rapid solvent evaporation. The solvent vapor pressure critically determines the evaporation rate and drying time. Thus, the solvent volatility plays a major role in the formation of nanostructures by influencing the phase separation process.

20.2.2.3 Ambient Parameters

The surrounding conditions such as temperature, humidity, pressure, and air velocity in the chamber may have a direct influence on the fiber diameter and morphology. For instance, pores are formed on the surface of the electrospun fibers because of huge

variations in humidity level [25, 26]. Further, humidity in the surroundings of the electrospinning determines the rate of evaporation of the solvents in the electrospinning solution [27, 28].

20.3 Lithium-Ion Batteries

Among the various existing energy storage technologies, rechargeable lithium-ion batteries are considered an effective solution to the increasing need for high-energy electrochemical power sources. As one of the most important energy storage systems, the Li-ion battery (LIB) has been used not only in portable electronics but also in power batteries for electric vehicles. To meet the demands of all-electric vehicles in the long term, researchers have been devoted to developing other battery systems with lithium metal as the anode material to improve the energy density, such as lithium-sulfur battery and lithium-oxygen battery.

Primary Li batteries have become commercial during the 1970s. Attempts to develop rechargeable Li batteries with Li-metal anodes have accompanied the R&D of Li batteries from their early stages. However, a few nearly commercial products of secondary Li (metal) batteries appeared during the early 1990s. From the early stages of R&D of Li-ion batteries, it was clear that transition metal oxides and sulfides can serve as excellent reversible cathode materials for rechargeable Li batteries [29, 30]. The Li-ion battery technology evolution, which enabled the commercialization of the rechargeable, high-energy density batteries that are conquering the market, emerged due to introduction of graphite as the anode material instead of Li-metal, and the use of lithiated transition metal oxide as cathode materials; $LiMO_2$ as the source of lithium in the cell [31]. Graphite-$LiCoO_2$ became the leading Li-ion battery systems that are being used in most of the portable electronic devices, like laptops, cellular phone, digital cameras, etc.

Lithium-ion battery consists of a cathode and an anode separated by an electrolyte containing dissociated lithium salts, which enable the transfer of lithium ions between the two electrodes, as illustrated in Fig. 20.2. The electrolyte is typically contained in a porous separator membrane that prevents the physical contact between the cathode and anode. When the battery is being charged, an external electrical power source injects electrons into the anode. At the same time, the cathode gives up some of its lithium ions, which move through the electrolyte to the anode. During this process, electricity is stored in the battery in the form of chemical energy. During discharging, the lithium ions move back to the cathode, enabling the release of electrons to the outer circuit to do the electrical work.

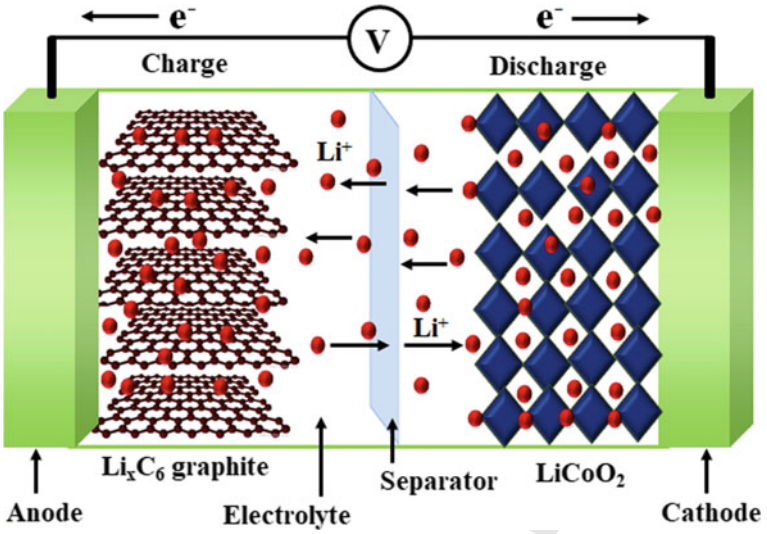

Fig. 20.2 Schematic representation of a lithium-ion battery

20.4 Electrospun Nanofiber-Based Lithium-Ion Batteries

Among the various existing energy storage technologies, lithium-ion batteries (LIBs) have become one of the most advanced rechargeable batteries for portable devices and more recently, for electric vehicles, because of their high energy density, negligible memory effect, and low self-discharge. Rechargeable lithium-ion batteries offer energy densities 2–3 times and power densities 5–6 times higher than the conventional nickel-cadmium (Ni-Cd) and nickel-metal hydride (Ni-MH) batteries, and as a result, they weigh less, take less space and deliver more energy [32–34]. In addition to high energy and power densities, lithium-ion batteries also have other advantages, such as high Coulombic efficiency, low self-discharge and high operating voltage [35].

At present, lithium-ion batteries depend on active powder materials such as graphite powder in the anode and $LiFePO_4$ powder in the cathode to store energy. However, powder materials have a long diffusion path for lithium ions and slow electrode reaction kinetics. The long migration pathways for the Li^+ of powder materials may lead to the large expansion volume during cycling, resulting in the low rate of performance and poor cyclability. Thus, electrodes with advanced nanostructured materials must be developed to obtain potential lithium-ion batteries that outperform current technologies and can be used in large-scale systems. Recently, the application of electrospun nanofibers in lithium-ion batteries has attracted much research attention. The electrospunned nanofiber-based electrodes exhibited the shorter diffusion pathways for the Li^+-ions in comparison with the powder materials. These electrodes

also showed an efficient electrochemical reaction kinetic due to a faster intercalation-deintercalation mechanism at the electrode-electrolyte interface. Besides, electrospun based materials are promising materials for LIBs because of their good electrochemical activity, high mechanical strength, and large specific surface area. Results also demonstrate that lithium-ion batteries using electrospun nanofiber cathodes have excellent overall performance including large capacity, high charge/discharge rate capability and extended cycle life. In this section, mixed oxide-based composites as cathodes for lithium-ion batteries are briefly discussed.

20.4.1 Mixed Nickel-Cobalt Dioxide, $LiNi_{1-Y}Co_yO_2$

In a series of research papers, Delmas group [36–39] and Zhecheva et al. [40] reported the structural details and physical properties of $LiNi_{1-y}Co_yO_2$ system and showed that there is an increased ordering as the cobalt concentration increases. The cobalt suppresses the migration of nickel to the lithium site in the mixed Li nickel/cobalt compounds. The same behavior was found in the system like Li nickel/manganese/cobalt oxides. Other ions, such as iron, do not have the same positive effect as cobalt. For example, in the case of the compound $LiNi_{1-y}Fe_yO_2$, the capacity is reduced with increasing iron [41]. The electronic conductivity is an important parameter which influences the properties of such layered oxides. Thus, cobalt substitution in $LiNiO_2$, as in $LiNi_{0.8}Co_{0.2}O_2$, reduces the conductivity [39]. Also, as lithium is removed from the phase $Li_xNi_{0.1}Co_{0.9}O_2$ or from Li_xCoO_2 the dramatic increase in conductivity was observed [42].

The studies have also shown that the addition of a little of a redox-inactive element such as magnesium as in case of $LiNi_{1-y}Mg_yO_2$ the capacity was reduced [43]. Similarly, in the case of substituted nickel oxides, such as $LiNi_{1-y-z}Co_yAl_zO_2$, the nickel is oxidized first to Ni^{4+} then the cobalt to Co^{4+} during charging these mixed oxides [44]. These are the prime candidates for the cathode of advanced lithium batteries for large-scale applications.

20.4.2 Lithium Manganese Dioxide, $LiMnO_2$

Lithium manganese dioxide ($LiMnO_2$) is a low-cost and environmentally friendly cathode material [45–47]. This can be prepared from three different approaches reported in the literature. The first approach includes ion exchange mechanism with the sodium compound, giving $LiMnO_2$, which was accomplished independently by Bruce and Armstrong [48] and Delmas et al. [49].

The second synthetic approach includes low temperatures preparation method. For example, the hydrothermal synthesis/decomposition of alkali permanganates, in the presence of lithium results in the composition $Li_{0.5}MnO_2.nH_2O$ [46, 49–51].

Mild warming causes the loss of water to give the desired layered Li_xMnO_2 and overheating to 150 °C leads to the formation of the spinel $LiMn_2O_4$.

The third approach includes electronic stabilization method. The idea behind this method is to make the electronic properties of Mn to be more cobalt-like by substitution of Mn with more electron-rich elements such as Ni [52]. The successful substitution of Mn by Ni and Co has been reported [53–55]. Spahr et al. [56] demonstrated a high capacity and reversibility for $LiNi_{0.5}Mn_{0.5}O_2$. More recently, the compounds $LiNi_{1-y-z}Mn_yCo_zO_2$ have been extensively investigated and found to have properties that qualify them as possible candidates for the replacement of $LiCoO_2$ [57–59]. In addition to their high lithiation capacities and reversibility, these compounds show higher thermal stabilities compared to the cobalt-free compounds.

20.4.3 Mixed Manganese-Cobalt Dioxide, $LiMn_{1-Y}Co_yO_2$

Bruce et al. [60] reported the synthesis and electrochemical performance of cobalt-substituted $LiMn_{1-y}Co_yO_2$. In such compounds, the partial substitution of manganese ions by cobalt, iron, or nickel was found to significantly increase the electronic conductivity of the manganese oxide. To obtain sufficiently dense material for conductivity measurement, the potassium analogs were synthesized at elevated temperatures with 10% of the manganese substitution. The study showed the enhanced conductivity by almost 2 orders of magnitude upon adding cobalt. These cobalt-substituted materials can also be prepared hydrothermally, and their cycling behavior is much improved over the cobalt-free compounds [61].

Doping elements other than cobalt have also been investigated, but substitution by nickel leads to a system where the manganese becomes the structure stabilizer and nickel is the electrochemically active ion. These compounds are thus best described as substituted nickel oxides in which the manganese remains in the tetravalent state and the nickel is redox-active between the +2 and +4 oxidation states. The manganese helps to stabilize the lattice and reduces the cost as well. Cobalt plays a critical role in controlling the ordering of the 3d ions in the structure.

20.4.4 Mixed Nickel-Manganese Dioxide, $LiNi_{1-Y}Mn_yO_2$, Multi-electron Redox Systems

Ammundsen and Davidson research groups studied the mixed metal compounds like Li–Mn–Cr–O_2 system [62, 63]. The lithium ions in the transition metal layer were found clustered around the manganese ions as in Li_2MnO_3, and the system can be considered as a solid solution of Li_2MnO_3 and $LiCrO_2$. Considering the toxicity of Cr(VI), this pioneering research provoked much thinking about other multi-electron redox reaction and is discussed here. The Dahn research group [64]

studied $LiNi_{1-y}Mn_yO_2$ phase system and reported a solid solution for $y \leq 0.5$ but a deterioration of the electrochemical behavior with increasing the manganese content. Spahr et al. [56] repeated the optimum electrochemical behavior for the composition $LiNi_{0.5}Mn_{0.5}O_2$. This compound is called as 550 material (0.5 Ni, 0.5 Mn, 0.0 Co).

Spahr et al. [56] prepared 550 compounds at 700 °C and reported the capacity of 150 mA h g^{-1} falling to 125 mA h g^{-1} after 25 cycles and to 75 mA h g^{-1} after 50 cycles. They also showed that the capacity and its retention increased as the synthesis temperature was increased from 450 to 700 °C. Similarly, Ohzuku et al. [65] prepared the 550 material at 1000 °C and reported a constant capacity of 150 mA h g^{-1} at 0.1 mA cm^{-2}. The 550 material, synthesized at 900 °C and quenched to room temperature, also showed a capacity exceeding 150 mA h g^{-1} for over 50 cycles in thin-film configuration [66]. A material formed at 1000 °C showed a lower capacity of ~ 120 mA h g^{-1} at 0.1 mA cm^{-2}; the capacity was increased to about 140 mA h g^{-1} by addition of 5% cobalt, aluminum or titanium [67]. This suggests that the synthesis temperature of 1000 °C may be too high, leading possibly to excess nickel in the lithium layer. This 550 compound can intercalate second lithium, particularly when some titanium is added, forms $yLiNi_{0.5}Mn_{0.5}O_2.(1\text{-}y)Li_2TiO_3$, which results from the reduction of Mn(IV) to Mn(II) [68].

In conclusion, the mixed nickel-manganese dioxides have the following cathode characteristics:

i. It has a capacity of ~ 180 mA h g^{-1} for at least 50 cycles under mild cycling condition,
ii. The synthesis temperature should be over 700 °C and less than 1000 °C, probably optimally ~ 900 °C,
iii. Additions of cobalt can reduce the level of nickel in the lithium layer,
iv. The lithium in the transition metal layer may be a necessary structural component,
v. Nickel is the electrochemically active ion, and
vi. The electronic conductivity needs to be increased.

20.4.5 Mixed Nickel-Manganese-Cobalt Dioxide, $LiNi_{1-Y-Z}Mn_yCo_zO_2$

The synthesis of mixed nickel-manganese-cobalt dioxides was first reported in 1999 by Liu et al. [69] and in 2000 by Yoshio et al. [52]. The addition of cobalt to $LiMn_{1\text{-}y}Ni_yO_2$ would stabilize the structure in a strictly two-dimensional pattern. Ohzuku et al. [57] synthesized the symmetric compound $LiNi_{0.33}Mn_{0.33}Co_{0.33}O_2$ at 1000 °C and reported a capacity of ~150 mA h g^{-1}. This compound will be hereafter referred to as 333 materials. The synthesis of these $LiNi_{1-y-z}Mn_yCo_zO_2$ compounds is typically accomplished using a modified mixed-hydroxide approach by reacting $Ni_{1-y-z}Mn_yCo_z(OH)_2$ with a lithium salt in air or oxygen as described in Liu's first synthesis at 750 °C [69].

The synthesis temperature has a profound effect on the composition. For example, for the composition $LiNi_{0.4}Mn_{0.4}Co_{0.2}O_2$, the sample prepared at 1000 °C when cooled rapidly to ambient temperatures has almost 10% Ni occupancy in the lithium layer. Kim et al. [70] also reported a high Ni content of 5.9% on the Li site for samples of the 333 compositions prepared at 950 °C. At 900 °C even with more cobalt than nickel in the material, there is still considerable nickel disorder, almost 2% more Ni in the lithium layer at 900 °C than at 800 °C for all compositions. This suggests that high temperature increases the disorder of the nickel ions and this could be reduced by slow cooling of the sample in an oxidizing environment. This will allow the partial reordering of the ions [71].

Although these materials show good electrochemical behavior, their electronic conductivity is still low for a high-rate cathode. The conductivity needs to be improved without the addition of excessive amounts of a conductor such as carbon black, which will reduce the volumetric energy storage capacity. There has also been a report [72] on the low packing density of powders which will also severely reduce the volumetric energy density. The conductivity of $LiNi_{0.5}Mn_{0.5}O_2$ was 6.2×10^{-5} S cm^{-1}; this increased on cobalt addition to 1.4×10^{-4} S cm^{-1} for $LiNi_{0.4}Mn_{0.4}Co_{0.2}O_2$ at 21 °C and 6.8×10^{-4} S cm^{-1} at 100 °C [73].

For the four oxides $Li_xNi_{1.02}O_2$, $Li_xNi_{0.89}Al_{0.16}O_2$, $Li_xNi_{0.70}Co_{0.15}O_2$, and $Li_xNi_{0.90}Mn_{0.10}O_2$, a structural transformation first to a spinel phase and then to a rock salt phase was found [74, 75] for lithium x values of 0.5 or less. The second transformation is accompanied by a loss of oxygen, and the first may be depending on the composition but usually when x is less than 0.5; the latter oxygen release occurs at a lower temperature as the lithium content decreases and as low as 190 °C for $Li_{0.3}Ni_{1.02}O_2$. The stability is improved on aluminum or cobalt substitution. The compound $Li_{0.1}NiO_2$ is reported [76] to lose weight at 200 °C forming a rock salt structure. The substitution of manganese for nickel appears to move the transition to the spinel to higher temperatures; thus, $Li_{0.5}Ni_{0.5}Mn_{0.5}O_2$ even after 3 days at 200 °C is still layered [77], but a spinel phase is formed above 400 °C and is stable to much higher temperatures for the 1:1 Ni:Mn lithium-free compound, eventually giving a mixture of spinel and nickel oxide in air and $NiO + Mn_3O_4$ in nitrogen [78]. The compounds $Li_{0.5}Ni_{0.4}Mn_{0.4}Co_{0.2}O_2$ and $Li_{0.5}Ni_{0.33}Mn_{0.33}Co_{0.33}O_2$ both begin to lose weight above 300 °C with major weight loss, 7–8%, only above 450 °C, which corresponds to reduction of Co(III) to Co(II) and any Ni(IV) to Ni(II); the manganese remains Mn(IV), and the structure begins to change to spinel by 350 °C, and the spinel phase is still present at 600 °C.

In conclusion, the mixed nickel-manganese-cobalt dioxides have the following cathode characteristics:

i. The synthesis temperature should be over 700 °C and less than 1000 °C, probably optimally ~ 900 °C,
ii. The cobalt reduces the number of nickel ions in the lithium layer,
iii. Nickel is the electrochemically active ion at low potentials,
iv. Cobalt is only active at the higher potentials,
v. The electronic conductivity need to be increased, and

vi. The optimum composition is still to be determined for energy storage, power capability, life-time, and cost considerations.

20.4.6 Lithium-Rich Mixed Metal Dioxides, $Li_{1+X}M_{1-X}O_2$

As explained in the case of chromium [79, 80] and cobalt [81] systems, excess lithium can be incorporated into the layered structure through a solid solution of Li_2MnO_3 and LMO_2, where M = Cr or Co. Yoshio et al. [82], Thackeray et al. [83, 84] and Dahn et al. [66] reported that the transition metal cation can also be nickel or manganese including mixtures such as $LiNi_{1-y}$ Co_yO_2 and Li_2MnO_3 can be replaced by related materials such as Li_2ZrO_3 and Li_2TiO_3. Li_2MnO_3 can be represented in the normally layered notation as $Li[Li_{1/3}Mn_{2/3}]O_2$. These solid solutions can thus be represented as $LiM_{1-y}[Li_{1/3}Mn_{2/3}]_yO_2$, where M can be, for example, Cr, Mn, Fe, Co, Ni, or mixtures thereof. Addition of extra lithium will tend to push the manganese away from trivalent to tetravalent, and thus minimizing the impact of any Jahn-Teller distortion coming from Mn^{3+}. The end-member Li_2MnO_3 which has been shown [85, 86] to exhibit unexpected electrochemical activity on charging as the manganese is already in the 4^+ oxidation state. This overcharging can be associated with two phenomena, removal of lithium with the concomitant loss of oxygen giving a defective oxygen lattice and the removal of lithium by decomposition of the electrolyte giving protons which can ion exchange for the lithium. The predominance of the mechanism depends on the temperature and chemical composition of the oxide lattice [87]. In both cases, the manganese oxidation state remains unchanged. Acid leaching of Li_2MnO_3 also results in the removal of lithium, and here again, both mechanisms of Li_2O removal [88, 89] and proton exchange [90] are believed to be operative. Acid leaching of the lithium stoichiometric compounds, such as $LiNi_{0.4}Mn_{0.4}Co_{0.2}O_2$, also results in the removal of lithium and a small amount of proton exchange. Thackeray et al. [91] showed that Li_2TiO_3 forms a solid solution with $LiNi_{0.5}Mn_{0.5}O_2$ and that the titanium helped allow the intercalation of second lithium into the structure [68]. Addition of some cobalt to these manganese-rich compounds was reported to help retain the capacity at higher discharge rates [92]. Magnesium has also been proposed as a stabilizing agent for manganese-rich materials [93]. The lithium excess content is one of the important parameters to be considered in addition to the nickel, cobalt and manganese ratios in designing the optimum composition for the ideal cathode. Each of these elements has a role to play. Manganese helps to stabilize the lattice; nickel acts as the electrochemically active member; cobalt helps in ordering the transition metals and thus increasing conductivity and the rate capability, and the lithium improves the capacity.

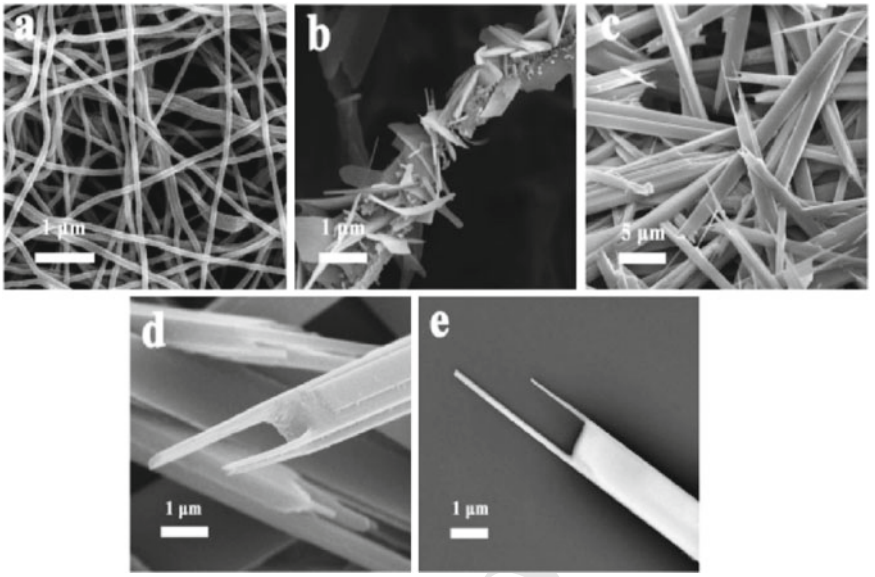

Fig. 20.3 Different magnifications SEM images of the precursor nanofibers (**a**), $K_2V_8O_{21}$ nanostructures annealed at 350 °C (**b**), and 500 °C (**c**–**e**). Adapted and reproduced from Ref. [94]

20.4.7 Electrospun Single-Crystalline Fork-like $K_2V_8O_{21}$

Anqiang et al. [94] reported the synthesis of single-crystalline fork-like potassium vanadate ($K_2V_8O_{21}$) by electrospinning method and a subsequent annealing process. A unique layer-by-layer stacked structure with fork-like morphology was seen in the SEM images as shown in Fig. 20.3. The prepared materials exhibit high specific discharge capacity and excellent cyclic stability with high specific discharge capacities of 200.2 and 131.5 mA h g^{-1} can be delivered at the current densities of 50 and 500 mA g^{-1}, respectively. Furthermore, the $K_2V_8O_{21}$ electrode exhibits excellent long-term cycling stability which maintains a capacity of 108.3 mA h g^{-1} after 300 cycles at 500 mA g^{-1}. These excellent results demonstrate their potential applications in next-generation high-performance lithium-ion batteries.

20.4.8 Lithium Iron Phosphate ($LiFePO_4$)—3D Carbon Nanofiber Composites

Dimesso et al. [95] reported the composite consist of $LiFePO_4$ as cathode material and deposited on carbon nanofiber 3D nonwovens prepared via electrospinning technique. The $LiFePO_4$ was prepared by Pechini-assisted sol-gel process. The cathode material was then coated on carbon nanofiber 3D nonwovens by soaking in

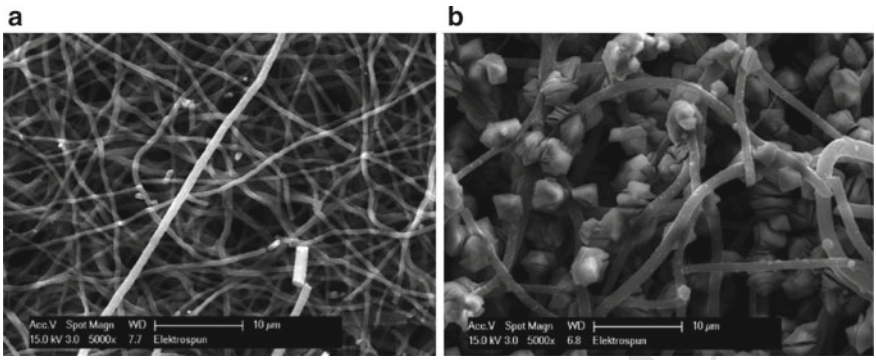

Fig. 20.4 The SEM images of **a** carbon nanofibers, **b** $LiFePO_4$/C nanofiber composites Adapted and reproduced from Ref. [95]. Copyright 2020 AIP Publishing

an aqueous solution containing lithium, iron salts and phosphates for 2–4 h at 70 °C. The composites were then annealed at 600 °C for 5 h under an inert atmosphere. The SEM images of the prepared composites are shown in Fig. 20.4 indicated a uniform coating of the carbon nanofibers and the uniform distribution of cauliflower-like crystalline structures all over the surface area of the carbon nanofibers. The electrochemical measurements on the composites showed good performances delivering a discharge specific capacity of 156 mA h g^{-1} at a discharging rate of C/25 and 152 mA h g^{-1} at a discharging rate of C/10 at ambient temperature.

20.5 Future Prospects and Conclusions

Lithium batteries have made a substantial and significant contribution in dominant rechargeable battery for consumer portable applications. Electrospinning is a versatile technique presents many opportunities in the enhancement of Li-ion battery performance by easy modifications of components. The literature explicitly showed the clear advantage of increased charge retention and achievable energy densities approaching the theoretical capacity of the active materials. The electrospun NMC/C fibers exhibited the higher capacities of ~ 200–250 mA h g^{-1} with energy densities of ~200 Wh kg^{-1}. Recent studies also demonstrated the advantages of nanofiber usage because of increased gravimetric storage capacities. A further potential advantage, in addition to higher gravimetric energy densities, is capacity retention. This is also an essential factor for short-term energy storage during high peak loads. There are notable potential gains in using fibrous cathodes, while some drawbacks require solutions. The next market opportunities mostly demand higher power capabilities at lower costs with enhanced safety. The developments on the area layered oxides and mixed transition metals replacing the cobalt system and proving enhanced safety with improved electrochemical performance. Though the material made of lithium iron

phosphate is a potentially low-cost cathode, the costs of the other cell components including the electrolyte, anode and the separators, need to be reduced.

In addition, the balance of the active material/C ratio is extremely important to achieve a proper volumetric and gravimetric energy density of the product with a suitable nanofibrous structure. The large volumetric energy density, resulting from the high porosity of nanofiber webs, restricts the application of fibrous cathodes in vehicles and some portable devices, and instead suggests the potential application of fibrous cathodes in stationary storage systems. Another drawback observed in laboratory experiment is the *in situ* synthesis of active material containing CNFs. The active material is often more brittle than fibers containing already-synthetized nanoparticles. These two challenges would impede industrial production.

References

1. Clark MD, Walker LS, Hadjiev VG, Khabashesku V, Corral EL, Krishnamoorti R, Cinibulk M (2015) Fast sol-gel preparation of silicon carbide-silicon oxycarbide nanocomposites. J Am Ceram Soc 94:4444–4452. https://doi.org/10.1111/j.1551-2916.2011.04707.x
2. Balde CP, Hereijgers BP, Bitter JH, Jong KP (2008) Sodium alanate nanoparticles—linking size to hydrogen storage properties. J Am Chem Soc 130:6761–6765. https://doi.org/10.1021/ja710667v
3. Li M, Wu X, Zeng J, Hou Z, Liao S (2015) Heteroatom doped carbon nanofibers synthesized by chemical vapor deposition as platinum electrocatalyst supports for polymer electrolyte membrane fuel cells. Electrochim Acta 182:351–360. https://doi.org/10.1016/j.electacta.2015.09.122
4. Reddy M, Beichen Z, Nicholette JLE, Kaimeng Z, Chowdari B (2011) Molten salt synthesis and its electrochemical characterization of Co_3O_4 for lithium batteries. Electrochem Solid State Lett 14:A79–A82. https://doi.org/10.1149/1.3556984
5. Reddy M, Yu C, Jiahuan F, Loh KP, Chowdari B (2012) Molten salt synthesis and energy storage studies on $CuCo_2O_4$ and $CuO{\cdot}Co_3O_4$. RSC Adv. 2:9619–9625. https://doi.org/10.1039/C2RA21033A
6. Reddy M, Khai V, Chowdari B (2015) Facile one pot molten salt synthesis of nano $(M_{1/2}Sb_{1/2}Sn)O_4$ (M = V, Fe, In). Mater Lett 140:115–118. https://doi.org/10.1016/j.matlet.2014.10.145
7. Wu Y, Reddy M, Chowdari B, Ramakrishna S (2013) Long-term cycling studies on electrospun carbon nanofibers as anode material for lithium ion batteries. ACS Appl Mater Interf 5:12175–12184. https://doi.org/10.1021/am404216j
8. Reddy M, Quan CY, Teo KW, Ho LJ, Chowdari B (2015) Mixed oxides, $(Ni_{1-x}Zn_x)Fe_2O_4$ ($x = 0, 0.25, 0.5, 0.75, 1$): Molten salt synthesis, characterization and its lithium-storage performance for lithium ion batteries. J Phys Chem C 119:4709–4718. https://doi.org/10.1021/jp5121178
9. Reddy M, Cherian CT, Ramanathan K, Jie KCW, Daryl TYW, Hao TY, Adams S, Loh KP, Chowdari BVR (2014) Molten synthesis of $ZnO.Fe_3O_4$ and Fe_2O_3 and its electrochemical performance. Electrochim Acta 118:75–80. https://doi.org/10.1016/j.electacta.2013.11.125
10. Sakunthala A, Reddy M, Selvasekarapandian S, Chowdari B, Selvin PC (2010) Synthesis of compounds, $Li(MMn_{11/6})O_4$ ($M = Mn_{1/6}, Co_{1/6}, (Co_{1/12}Cr_{1/12}), (Co_{1/12}Al_{1/12}), (Cr_{1/12}Al_{1/12})$) by polymer precursor method and its electrochemical performance for lithium-ion batteries. Electrochim Acta 55:4441–4450. https://doi.org/10.1016/j.electacta.2010.02.080
11. Reddy M, Sakunthala A, Selvashekara Pandian S, Chowdari B (2013) Preparation, comparative energy storage properties, and impedance spectroscopy studies of environmentally friendly

cathode, $Li(MMn_{11/6})O_4$ (M = $Mn_{1/6}$, $Co_{1/6}$, $(Co_{1/12}Cr_{1/12})$). J Phy Chem C 117:9056–9064. https://doi.org/10.1021/jp309180k
12. Prabu M, Reddy M, Selvasekarapandian S, Rao GS, Chowdari B (2013) (Li, Al)-co-doped spinel, $Li(Li_{0.1}Al_{0.1}Mn_{1.8})O_4$ as high performance cathode for lithium ion batteries. Electrochim Acta 88:745–755. https://doi.org/10.1016/j.electacta.2012.10.011
13. Zhao X, Reddy M, Liu H, Ramakrishna S, Rao GS, Chowdari B (2012) Nano $LiMn_2O_4$ with spherical morphology synthesized by a molten salt method as cathodes for lithium ion batteries. RSC Adv 2:7462–7469. https://doi.org/10.1039/C2RA01110G
14. Reddy M, Raju MS, Sharma N, Quan P, Nowshad SH, Emmanuel H-C, Peterson V, Chowdari B (2011) Preparation of $Li_{1.03}Mn_{1.97}O_4$ and $Li_{1.06}Mn_{1.94}O_4$ by the polymer precursor method and X-ray, neutron diffraction and electrochemical studies. J Electrochem Soc 158:A1231–A1236. https://doi.org/10.1149/2.074111jes
15. Reddy M, Cheng H, Tham J, Yuan C, Goh H, Chowdari B (2012) Preparation of $Li(Ni_{0.5}Mn_{1.5})O_4$ by polymer precursor method and its electrochemical properties. Electrochim Acta 62:269–275. https://doi.org/10.1016/j.electacta.2011.12.029
16. Ashammakhi N, Ndreu A, Piras AM, Nikkola L, Sindelar T, Ylikauppila H, Harlin A, Gomes ME, Neves NM, Chiellini E, Chiellini F, Hasirci V, Redl H, Reis RL (2006) Biodegradable nanomats produced by electrospinning: Expanding multifunctionality and potential for tissue engineering. J Nanosci Nanotechnol 6:2693–2711. https://doi.org/10.1166/jnn.2007.485
17. Reneker DH, Yarin AL (2008) Bending instability of electrically charged liquid jets of polymer solutions in electrospinning. Polymer 49:2387–2425. https://doi.org/10.1063/1.373532
18. Deitzel JM, Kleinmeyer J, Harris D, Tan NCB (2001) The effect of processing variables on the morphology of electrospun nanofibers and textiles. Polymer 42(1):261–272. https://doi.org/10.1016/S0032-3861(00)00250-0
19. Megelski S, Stephens JS, Chase DB, Rabolt JF (2002) Micro- and nanostructured surface morphology on electrospun polymer fibers. Macromolecules 35(22):8456–8466. https://doi.org/10.1021/ma020444a
20. Baumgarten PK (1971) Electrostatic spinning of acrylic microfibers. J Colloid Interf Sci 36(1):71–79. https://doi.org/10.1016/0021-9797(71)90241-4
21. Buchko CJ, Chen LC, Shen Y, Martin DC (1999) Processing and microstructural characterization of porous biocompatible protein polymer thin films. Polymer 40(26):7397–7407. https://doi.org/10.1016/S0032-3861(98)00866-0
22. Eda G, Shivkumar S (2006) Bead structure variations during electrospinning of polystyrene. J Mater Sci 41(17):5704–5708. https://doi.org/10.1007/s10853-006-0069-9
23. Tao J, Shivkumar S (2007) Molecular weight dependent structural regimes during the electrospinning of PVA. Mater Lett 61(11–12):2325–2328. https://doi.org/10.1016/j.matlet.2006.09.004
24. Fridrikh SV, Yu JH, Brenner MP, Rutledge GC (2003) Controlling the fiber diameter during electrospinning. Phys Rev Lett 90(14):144502(1–4). https://doi.org/10.1103/PhysRevLett.90.144502
25. Nezarati RM, Eifert MB, Hernandez EC (2012) Effects of humidity and solution viscosity on electrospun fiber morphology. Tissue Eng Part C 19:810–819. https://doi.org/10.1089/ten.tec.2012.0671
26. Casper CL, Stephens JS, Tassi NG, Chase DB, Rabolt JF (2004) Controlling surface morphology of electrospun polystyrene fibers: effect of humidity and molecular weight in the electrospinning process. Macromolecules 37:573–578. https://doi.org/10.1021/ma0351975
27. Raghavan BK, Coffin DW (2011) Control of inter-fiber fusing for nanofiber webs via electrospinning. J Eng Fibers Fabr 6:1–5. https://www.jeffjournal.org/papers/Volume6/6.4.1Coffin.pdf
28. Htike HH, Chen L, Sachiko S (2012) The effect of relative humidity on electrospinning of poly(vinyl alcohol) with soluble eggshell membrane. J Textil Eng 58:9–12. https://doi.org/10.4188/jte.58.9
29. Gabano JP (1983) Lithium batteries. Academic Press, London and New York, 467. https://scholar.google.co.il/citations?user=EO-B1RMAAAAJ&hl=iw

30. Nazri GA, Pistoia G (2009) Lithium batteries: Science and technology. Springer. https://www.springer.com/gp/book/9781402076282
31. Scrosati B (1993) Insertion compounds for lithium rocking chair batteries: the electrochemistry of novel materials. VCH Publishers 3:111–137. https://d-nb.info/941450163/04
32. Tarascon M, Armand M (2001) Issues and challenges facing rechargeable lithium batteries. Nature 414:359–367. https://doi.org/10.1038/35104644
33. Long JW, Dunn B, Rolison DR, White HS (2004) Three-dimensional battery architectures. Chem Rev 104:4463–4492. https://doi.org/10.1021/cr020740l
34. Ji L, Zhang X (2008) Ultrafine polyacrylonitrile/silica composite fibers via electrospinning. Mater Lett 62:2165–2168. https://doi.org/10.1016/j.matlet.2007.11.051
35. Guo YG, Hu JS, Wan LJ (2008) Nanostructured materials for electrochemical energy conversion and storage devices. Adv Mater 20:2878–2887. https://doi.org/10.1002/adma.200800627
36. Rougier A, Saadouane I, Gravereau P, Willmann P, Delmas C (1996) Effect of cobalt substitution on cationic distribution in $LiNi_{1-y}$ Co_yO_2 electrode materials. Solid State Ionics 90:83–90. https://doi.org/10.1016/S0167-2738(96)00370-0
37. Saardoune I, Delmas C (1996) On the $Li_xNi_{0.8}Co_{0.2}O_2$ System. J Solid State Chem 136:8–15. https://doi.org/10.1006/jssc.1997.7599
38. Saadoune I, Menetrier M, Delmas C (1997) Redox processes in $Li_xNi_{1-y}Co_yO_2$ cobalt-rich phases. J Mater Chem 7:2505–2511. https://doi.org/10.1039/A703368K
39. Saadoune I, Delmas C (1996) $LiNi_{1-y}Co_yO_2$ positive electrode materials: relationships between the structure, physical properties and electrochemical behaviour. J Mater Chem 6:193–199. https://doi.org/10.1039/JM9960600193
40. Zhecheva E, Stoyanova R (1993) Stabilization of the layered crystal structure of $LiNiO_2$ by co-substitution. Solid State Ionics 66:143–149. https://doi.org/10.1016/0167-2738(93)90037-4
41. Prado G, Rougier A, Fournes L, Delmas C (2000) Electrochemical behavior of iron-substituted lithium nickelate. J Electrochem Soc 147:2880–2887. https://doi.org/10.1149/1.1393620
42. Imanishi N, Fujiyoshi M, Takeda Y, Yamamoto O, Tabuchi M (1999) Preparation and Li-NMR study of chemically delithiated $Li_{1-x}CoO_2$ ($0 < x < 0.5$). Solid State Ionics 118:121–128. https://doi.org/10.1016/S0167-2738(98)00441-X
43. Pouillerie C, Croguennec L, Delmas C (2000) The $Li_xNi_{1-y}Mg_yO_2$ ($y = 0.05, 0.10$) system: structural modifications observed upon cycling. Solid State Ionics 132:15–29. https://doi.org/10.1016/S0167-2738(00)00699-8
44. Nakai I, Nakagome T (1998) In-situ transmission X-ray absorption fine structure analysis of the Li deintercalation process in Li(Ni0.5Co0.5)O2. Electrochem Solid State Lett 1:259–261. https://doi.org/10.1149/1.1390705
45. Delmas C, Capitaine F (1996) Abstracts of the 8th international meeting, lithium batteries. Electrochemical Society, Pennington, NJ
46. Chen R, Whittingham MS (1997) Cathodic behavior of alkali manganese oxides from permanganate. J Electrochem Soc 144:L64–L67. https://doi.org/10.1149/1.1837554
47. Armstrong AR, Bruce PG (1996) Synthesis of layered $LiMnO_2$ as an electrode for rechargeable lithium batteries. Nature 381:499–500. https://doi.org/10.1149/1.1837554
48. Capitaine F, Gravereau P, Delmas C (1996) A new variety of $LiMnO_2$ with a layered structure. Solid State Ionics 89:197–202. https://doi.org/10.1016/0167-2738(96)00369-4
49. Chen R, Zavalij PY, Whittingham MS (1997) New manganese oxides by hydrothermal reaction of permanganates. Mater Res Soc Proc 453:653. https://doi.org/10.1557/PROC-453-653
50. Chen R, Zavalij P, Whittingham MS (1996) Hydrothermal synthesis and characterization of $K_xMnO_2{\cdot}yH_2O$. Chem Mater 8:1275. https://doi.org/10.1021/cm950550+
51. Chen R, Chirayil T, Whittingham MS (1996) The hydrothermal synthesis of sodium manganese oxide and a lithium vanadium oxide. Solid State Ionics 1:86–88. https://doi.org/10.1016/0167-2738(96)00086-0
52. Yoshio M, Yamato K, Itoh J, Noguchi H, Okada M, Mouri T (1994) Preparation and properties of $LiCo_yMn_xNi_{1-x-y}O_2$ as a cathode for lithium ion batteries. Electrochem Soc Proc 251:28–94. https://doi.org/10.1016/S0378-7753(00)00407-9

53. Nitta Y, Okamura K, Haraguchi K, Kobayashi S, Ohta A (1995) Crystal structure study of $LiNi_{1-x}Mn_xO_2$. J Power Sour 54:511–515. https://doi.org/10.1016/0378-7753(94)02137-R
54. Armstrong A, Gitzendanner R (1998) The intercalation compound $Li(Mn_{0.9}Co_{0.1})O_2$ as a positive electrode for rechargeable lithium batteries. Chem Commun 17:1833–1834. https://doi.org/10.1039/A803741H
55. Numata K, Yamanaka S (1999) Preparation and electrochemical properties of layered lithium-cobalt-manganese oxides. Solid State Ionics 118:117–120. https://doi.org/10.1016/S0167-2738(98)00425-1
56. Spahr ME, Novak P, Schnyder B, Haas O, Nesper R (1998) Characterization of layered lithium nickel manganese oxides synthesized by a novel oxidative coprecipitation method and their electrochemical performance as lithium insertion electrode materials. J Electrochem Soc 145:1113–1121. https://doi.org/10.1149/1.1838425
57. Ohzuku T, Makimura Y (2001) Layered lithium insertion material of $LiCo_{1/3}Ni_{1/3}Mn_{1/3}O_2$ for lithium-ion batteries. Chem Lett 30:642–643. https://doi.org/10.1246/cl.2001.642
58. Lu Z, MacNeil DD, Dahn JR (2001) Layered Li [Ni_xCo_1—$2xMnx]O_2$ cathode materials for lithium-ion batteries. Electrochem Solid State Lett 4:A200–A203. https://doi.org/10.1149/1.1413182
59. Wang Z, Sun Y, Chen L, Huang X (2004) Electrochemical characterization of positive electrode material LiNi1/3Co1/3Mn1/3O2 and compatibility with electrolyte for Lithium-ion batteries. J Electrochem Soc 151:A914–A921. https://doi.org/10.1149/1.1740781
60. Armstrong AR, Paterson AJ, Robertson AD, Bruce PG (2002) Nonstoichiometric layered $Li_xMn_yO_2$ with a high capacity for lithium intercalation/deintercalation. Chem Mater 14:710–719. https://doi.org/10.1021/cm010382n
61. Zhang F, Whittingham MS (2000) Electrochemistry of the layered manganese dioxides: a xMn1—y(Co, Ni, Fe)yO2 (A = Li, K) rate effects. Electrochem Solid State Lett 3:309–311. https://doi.org/10.1149/1.1391132
62. Grincourt Y, Storey C, Davidson IJ (2001) Lithium ion cells using a new high capacity cathode. J Power Source 97–98:711–713. https://doi.org/10.1016/S0378-7753(01)00750-9
63. Storey C, Kargina I, Grincourt Y, Davidson IJ, Yoo YC, Seung DY (2001) Electrochemical characterization of a new high capacity cathode. J Power Sour 97–98:541–544. https://doi.org/10.1016/S0378-7753(01)00692-9
64. Rossen E, Jones CDW, Dahn JR (1992) Structure and electrochemistry of $Li_xMn_yNi_{1-y}O_2$. Solid State Ionics 57:311–318. https://doi.org/10.1016/0167-2738(92)90164-K
65. Ohzuku T, Makimura Y (2001) Layered lithium insertion material of $LiNi_{1/2}Mn_{1/2}O_2$: a possible alternative to $LiCoO_2$ for advanced lithium-ion batteries Chem. Lett. 30:744–745. https://doi.org/10.1246/cl.2001.744
66. Lu Z, MacNeil DD, Dahn JR (2001) Layered cathode materials Li [Ni_xLi (1/3–2x/3)Mn(2/3–x/3)]O2 for lithium-ion batteries. Electrochem Solid State Lett 4:A191–A194. https://doi.org/10.1149/1.1407994
67. Kang S-H, Kim J, Stoll ME, Abraham D, Sun YK, Amine K (2002) Layered $Li(Ni_{0.5-x}Mn_{0.5-x}M_{2x}')O_2$ (M′ = Co, Al, Ti; x = 0, 0.025) cathode materials for Li-ion rechargeable batteries. J Power Sour 112:41–48. https://doi.org/10.1016/S0378-7753(02)00360-9
68. Johnson CS, Kim JS, Kropf AJ, Kahaian AJ, Vaughey JT, Thackeray MM (2002) The role of Li_2MO_2 structures (M=metal ion) in the electrochemistry of $(x)LiMn_{0.5}Ni_{0.5}O_2{\cdot}(1-x)Li_2TiO_3$ electrodes for lithium-ion batteries. Electrochem Commun 4:492–498. https://doi.org/10.1016/S1388-2481(02)00346-6
69. Liu Z, Yu A, Lee JY (1999) Synthesis and characterization of $LiNi_{1-x-y}Co_xMn_yO_2$ as the cathode materials of secondary lithium batteries. J Power Sour 81–82:416–419. https://doi.org/10.1016/S0378-7753(99)00221-9
70. Kim JM, Chung HT (2004) The first cycle characteristics of $Li[Ni_{1/3}Co_{1/3}Mn_{1/3}]O_2$ charged up to 4.7 V. Electrochim Acta 49:937–944. https://doi.org/10.1016/j.electacta.2003.10.005
71. Jouanneau S, Eberman KW, Krause LJ, Dahn JR (2003) Synthesis, characterization and electrochemical behavior of improved Li [NixCo1 − 2_xMn_x] O2 ($0.1 \leq x \leq 0.5$). J Electrochem Soc 150:A1637–A1642. https://doi.org/10.1149/1.1622956

72. Jouanneau S, Macneil DD, Lu Z, Beattie SD, Murphy G, Dahn JR (2003) Morphology and safety of Li [$Ni_xCo1–2_xMn_x$]O2($0 \leq x \leq 1/2$). J Electrochem Soc 150:A1299–A1304. https://doi.org/10.1149/1.1602077
73. Ngala JK, Chernova NA, Ma M, Mamak M, Zavalij PY, Whittingham MS (2004) The synthesis, characterization and electrochemical behavior of the layered $LiNi_{0.4}Mn_{0.4}Co_{0.2}O_2$ compound. J Mater Chem 14:214–220. https://doi.org/10.1039/B309834F
74. Guilmard M, Croguennec L, Delmas C (2003) Thermal stability of lithium nickel oxide derivatives. Part I: $Li_xNi_{1.02}O_2$ and $Li_xNi_{0.89}Al_{0.16}O_2$ ($x = 0.50$ and 0.30). Chem Mater 15:4476–4483. https://doi.org/10.1021/cm030059f
75. Guilmard M, Croguennec L, Delmas C (2003) Thermal stability of lithium nickel oxide derivatives Part II: $Li_xNi_{0.70}Co_{0.15}Al_{0.15}O_2$ and $Li_xNi_{0.90}Mn_{0.10}O_2$ ($x = 0.50$ and 0.30). Comparison with $Li_xNi_{1.02}O_2$ and $Li_xNi_{0.89}Al_{0.16}O_2$. Chem Mater 15:4484–4493. https://doi.org/10.1021/cm030340u
76. Arai H, Sakurai Y (1999) Characteristics of $LixNiO_2$ obtained by chemical delithiation. J Power Sour 80–81:401–405. https://doi.org/10.1016/S0378-7753(99)00115-9
77. Choi S, Manthiram A (2000) Synthesis and electrode properties of metastable $Li_2Mn_4O_9$- δ spinel oxides. J Electrochem Soc 147(5):1623–1629. https://scholar.google.com/citations?hl=en&user=DGy5QdUAAAAJ&view_op=list_works&sortby=pubdate
78. Chen R, Zavalij PY, Whittingham MS, Greedan JE, Raju NP, Bieringer M (1999) The hydrothermal synthesis of the new manganese and vanadium oxides, $NiMnO_3H$, MAV_3O_7 and $MA_{0.75}V_4O_{10}.0.67H_2O$ (MA=CH_3NH_3). J Mater Chem 9:93–100. https://doi.org/10.1039/a805312j
79. Ammundsen B, Desilvestro H, Paulson JM, Steiner R, Pickering PJ (2000) 10th international meeting on lithium batteries, Italy, 2000. Electrochemical Society, Pennington, NJ
80. Storey C, Kargina I, Grincourt Y, Davidson IJ, Yoo Y, Seung DY (2000) 10th International meeting on lithium batteries, Italy, Electrochemical Society: Pennington, NJ, vol 10, abstract 234
81. Numata K, Sakaki C, Yamanaka S (1999) Synthesis and characterization of layer structured solid solutions in the system of $LiCoO_2$-Li_2MnO_3. Solid State Ionics 117:257–263. https://doi.org/10.1016/S0167-2738(98)00417-2
82. Yoshio M, Noguchi H, Itoh J, Okada M, Mouri T (2000) Preparation and properties of $LiCo_yMn_xNi_{1-x-y}O_2$ as a cathode for lithium ion batteries. J Power Sour 90:176–181. https://doi.org/10.1016/S0378-7753(00)00407-9
83. Thackeray MM, Johnson CS, Amine K, Kim J (2004) Lithium metal oxide electrodes for lithium cells and batteries. U.S. Patent 6,677,082
84. Thackeray MM, Johnson CS, Amine K, Kim J (2004) Lithium metal oxide electrodes for lithium cells and batteries. U.S. Patent 6,680,143
85. Robertson AD, Bruce PG (2002) The origin of electrochemical activity in Li_2MnO_3. Chem Commun 2790–2791. http://doi.org/10.1039/b207945c
86. Robertson AD, Bruce PG (2003) Mechanism of electrochemical activity in Li_2MnO_3. Chem Mater 15:1984–1992. https://doi.org/10.1021/cm030047u
87. Armstrong AR, Bruce PG (2004) Electrochemistry beyond Mn4 + in LixMn1 − yLiy O2 Electrochem. Solid State Lett. 7:A1–A4. https://doi.org/10.1149/1.1625591
88. Russouw MH, Thackeray MM (1991) Lithium manganese oxides from Li_2MnO_3 for rechargeable lithium battery applications. Mater Res Bull 26:463–473. https://doi.org/10.1016/0025-5408(91)90186-P
89. Russouw MH, Liles DC, Thackeray MM (1993) Synthesis and structural characterization of a novel layered lithium manganese oxide, $Li_{0.36}Mn_{0.91}O_2$, and its lithiated derivative, $Li_{1.09}Mn_{0.91}O_2$. J Solid State Chem 104:464–466. https://doi.org/10.1006/jssc.1993.1182
90. Paik Y, Grey CP, Johnson CS, Kim JS, Thackeray MM (2002) Lithium and deuterium NMR studies of acid-leached layered lithium manganese oxides. Chem Mater 14:5109–5115. https://doi.org/10.1021/cm0206385
91. Kim JS, Johnson CS, Thackeray MM (2002) Layered $xLiMO_2 \cdot (1-x)Li_2M'O_3$ electrodes for lithium batteries: a study of $0.95LiMn_{0.5}Ni_{0.5}O_2 \cdot 0.05Li_2TiO_3$. Electrochem Commun 4:205–209. https://doi.org/10.1016/S1388-2481(02)00251-5

644 92. Kim JH, Park CW, Sun YK (2003) Synthesis and electrochemical behavior of
645 $Li[Li_{0.1}Ni_{0.35-x/2}Co_xMn_{0.55-x/2}]O_2$ cathode materials. Solid State Ionics 164:43–49. https://
646 doi.org/10.1016/j.ssi.2003.08.003
647 93. Lee CW, Sun YK, Prakash J (2004) A novel layered Li $[Li_{0.12}Ni_zMg_{0.32-z}Mn_{0.56}]O_2$ cathode
648 material for lithium-ion batteries. Electrochim Acta 49:4425–4432. https://doi.org/10.1016/j.
649 electacta.2004.04.033
650 94. Hao P, Zhu T, Su Q, Lin J, Cui R, Cao X, Wang Y, Pan A (2018) Electrospun single crys-
651 talline fork-like $K_2V_8O_{21}$ as high-performance cathode materials for lithium-ion batteries.
652 Front Chem 6:195(1–9). https://doi.org/10.3389/fchem.2018.00195
653 95. Dimesso L, Spanheimer C, Jaegermann W, Zhang Y, Yarin AL (2012) $LiFePO_4$-3D carbon
654 nanofiber composites as cathode materials for Li-ions batteries. J Appl Phys 111:064307.
655 https://doi.org/10.1063/1.3693575